Research Article

Journal of PeptideScience

Received: 30 September 2010 Revised: 28 October 2010 Accepted: 4 November 2010 Published online in Wiley Online Library: 4 February 2011

(wileyonlinelibrary.com) DOI 10.1002/psc.1340

The thin line between cell-penetrating and antimicrobial peptides: the case of Pep-1 and Pep-1-K‡

Sara Bobone,[a] Alessandro Piazzon,[a] Barbara Orioni,[a] Jens Z. Pedersen,[b] Yong Hai Nan,[c] Kyung-Soo Hahm,[c,d] Song Yub Shin[c,d] and Lorenzo Stella[a]*

Cell-penetrating peptides (CPPs) are cationic oligopeptides able to translocate across biological membranes without perturbing them, while antimicrobial peptides (AMPs) kill bacteria mainly by disrupting their membranes. The two peptide classes share several characteristics (charge, amphipathicity, helicity, and length), and therefore the molecular properties discriminating between the two different bioactivities are not clear. Pep-1-K (KKTWWKTWWTKWSQPKKKRKV) is a new AMP derived from the widely studied CPP Pep-1 (KETWWETWWTEWSQPKKKRKV), or 'Chariot', known for its ability to carry large cargoes across biological membranes. Pep-1-K was obtained from Pep-1 by substituting the three Glu residues with Lys, to increase its cationic character. Previous studies showed that these modifications endow Pep-1-K with a potent antimicrobial activity, with MICs in the low micromolar range. Here, we characterized the interaction of Pep-1 and Pep-1-K with model membranes to understand the reason for the antimicrobial activity of Pep-1-K. The data show that this peptide causes vesicle aggregation, perturbs membrane order, and induces the leakage of ions, but not of larger solutes, while these effects were not observed for Pep-1. These differences are likely due, at least in part, to the higher affinity of Pep-1-K toward anionic bilayers, which mimick the composition of bacterial membranes.

Keywords: fluorescence spectroscopy; liposomes; water–membrane partition; ion leakage

Introduction

Several peptides exert their biological activity by interacting with cell membranes [1]. The two most prominent classes of such peptides are antimicrobial peptides (AMPs) and cell-penetrating peptides (CPPs). AMPs are an essential component of the innate defense system of most organisms and were first isolated in the 1980s by testing biological samples for antibacterial activity [2–4]. These peptides have multiple functions, including chemotactic and immunomodulatory roles [5,6] but most of them kill bacteria by perturbing the permeability of their cellular membranes [7,8]. For this reason, they are intensely investigated as a possible solution to the problem of drug-resistant bacteria [9,10]. CPPs, on the other hand, were initially identified (approximately in the same years) by observing the ability of some proteins, such as the *Drosophila Antennapedia* transcription factor or the HIV-1 Tat-transactivating protein, to translocate across biological membranes [11,12]. Short peptides derived from these proteins (penetratin and TAT peptides, respectively) were shown to maintain the same activity and to be able to deliver hydrophilic and macromolecular cargoes inside eukaryotic cells, without causing significant damage to their membranes [13,14]. Therefore, they have a huge potential for gene and drug delivery applications [15].

Due to their different origin, and to the different activities for which AMPs and CPPs were isolated and tested (antibacterial activity in one case and cell-penetrating activity in eukaryotic cells in the other), they have been considered as two distinct classes of peptides. From the structural point of view, there are no conserved features in each of the two classes, except for a few general properties, that, quite surprisingly, are common to AMPs and CPPs: both are short, amphiphilic and cationic, and they often attain a helical structure when associated to membranes. Therefore, a question naturally arises: what specifies the different activities of these peptides, or even are these activities actually distinct [16]? Indeed, when some CPPs were eventually tested for their antibacterial or membranolytic activity, the results surprisingly showed that CPPs were also able to penetrate bacterial membranes [17,18]. However, while they do not damage eukaryotic cells, many of them are membranolytic in bacteria or in model membranes mimicking the bacterial bilayer composition. For instance, pVEC was shown to kill bacteria by permeabilizing their membranes [17,18] and also transportan 10 (TP10) induces permeabilization of model membranes [19] and is bactericidal [17]. Although a

* *Correspondence to: Lorenzo Stella, Department of Chemical Sciences and Technologies, University of Rome Tor Vergata, Rome, Italy. E-mail: stella@stc.uniroma2.it*

a *Department of Chemical Sciences and Technologies, University of Rome Tor Vergata, Rome, Italy*

b *Department of Biology, University of Rome Tor Vergata, Rome, Italy*

c *Department of Bio-Materials, Graduate School and Research Center for Proteineous Materials, Chosun University, Gwangju 501-759, Republic of Korea*

d *Department of Cellular & Molecular Medicine, School of Medicine, Chosun University, Gwangju 501-759, Republic of Korea*

‡ *Special issue devoted to contributions presented at the 12th Naples Worshop on Bioactive Peptides and 2nd Italy-Korea Symposium on Antimicrobial Peptides, 4–7 June 2010, Naples, Italy.*

first report suggested that penetratin and TAT peptides did not permeabilize model membranes [20], more recent studies indicate that they actually do form pores [21–23]. Indeed, both penetratin [18,24] and TAT peptides [22] were shown to be antimicrobial, with a MIC in the micromolar range. Similar results were obtained for the artificial peptide MAP [18]. On the other hand, while most AMPs exert their activity by perturbing the bacterial membrane, some of them are known to penetrate inside bacterial cells and to act on intracellular targets. The most prominent example of these AMPs is buforin [25], but many other exist [26]. However, even membrane-perturbing AMPs, such as magainin, were shown to penetrate into eukaryotic cells [27].

For all these reasons, AMPs and CPPs might be more similar to each other than previously thought, and they could be grouped together in a more general class of 'membrane-active' peptides [16]. However, it remains to be clarified which are the structural features responsible for each of the two activities. Under this respect, the CPP Pep-1 is an illuminating example. Pep-1, or 'Chariot' (KETWWETWWTEWSQPKKKRKV), was designed by combining a hydrophobic, Trp-rich segment (KETWWETWWTEW) and a nuclear localization sequence, rich in charged residues (KKKRKV), separated by a Pro-containing spacer (SQP) [28]. The amphiphilic Pep-1 composition allows it to interact with lipid bilayers [29] and to form non-covalent aggregates with cargo molecules, stabilized by both hydrophobic and electrostatic interactions [30]. Pep-1 has a strong cell-penetrating activity, and although the exact mechanism by which it is able to transport proteins or peptides inside cells is still debated, a non-endocytotic pathway seems likely. Although the involvement of pore formation in the translocation process is controversial [31,32], it is now established that Pep-1 has some ability to perturb membrane permeability, at least at high concentrations and in the presence of a transmembrane potential. At very high concentrations it even becomes toxic, and it has been shown to have a weak antibacterial activity [33,34].

Starting from these observations, some of us designed a Pep-1 analog, called Pep-1-K in which all negatively charged residues where modified to Lys (KKTWWKTWWTKWSQPKKKRKV), with the aim of making it more similar to AMPs, which usually have a high cationic charge [33]. Indeed, Pep-1-K exhibited a strong antimicrobial activity, with MICs in the low micromolar range. The exact mechanism of antimicrobial activity of this analog remains to be clarified, as it was shown to cause membrane depolarization in bacteria, but not leakage of a fluorescent dye from liposomes [33]. These intriguing results raise a number of questions: do the sequence differences between Pep-1 and Pep-1-K influence only the antimicrobial activity of the two peptides or also their cell-penetrating properties? What is the mechanism of the antibacterial activity of Pep-1-K? More specifically, is membrane depolarization caused directly by Pep-1-K association to the bacterial surface or is it just a consequence of some other effect of the peptide on the cell metabolism? Last, but not least, what are the causes of the switch in activity between Pep-1 and Pep-1-K?

In this article, we address all these issues, by characterizing the interaction of Pep-1 and Pep-1-K with cells and model membranes. Our results indicate that the different activity of the two peptides is influenced by a higher affinity of Pep-1-K toward bacterial membranes, which allows this analog to reach the threshold membrane-bound concentration needed to cause the formation of small membrane defects, producing the leakage of ions but not of larger solutes.

Materials and Methods

Materials

All phospholipids were purchased from Avanti Polar Lipids (Alabaster, AL, USA). Spectroscopic grade methanol and chloroform were purchased from Carlo Erba Reagenti (Milano, Italy). Fmoc(9-fluorenylmethoxycarbonyl)-Val-Wang-resin, Fmoc-amino acids, and other reagents for peptide synthesis were purchased from Calbiochem-Novabiochem (La Jolla, CA, USA). Fluorophore sodium-binding benzofuran isophthalate (SBFI) was purchased from Invitrogen (Eugene, OR, USA). Fluorescein isothiocyanate (FITC) and 1,6-diphenyl-1,3,5-hexatriene (DPH) were supplied from Sigma-Aldrich (St. Louis, MO, USA).

Peptide Synthesis

Pep-1 and Pep-1-K and their FITC-labeled peptides were prepared by the standard Fmoc-based solid-phase method. *N*,*N*′-dicyclohexylcarbodiimide and *N*-hydroxybenzotriazole were used as coupling reagents, and tenfold excess Fmoc-amino acids were added during every coupling cycle. FITC was linked to the *N*-terminus of Pep-1 and Pep-1 K through an aminocaproic spacer. After cleavage and deprotection with a mixture of trifluoroacetic acid/water/thioanisole/phenol/ethanedithiol/triisopropylsilane (81.5 : 5 : 5 : 5 : 2.5 : 1, v/v) for 2 h at room temperature, the crude peptides were repeatedly extracted with diethyl ether and purified by HPLC on a preparative (15 µm, 20 mm × 250 mm) C_{18} Vydac column using an appropriate 0–80% water/acetonitrile gradient in the presence of 0.05% trifluoroacetic acid. The final purity of the peptides (>98%) was assessed by HPLC on a Vydac C_{18} reversed-phase analytical column (5 µm, 4.6 mm × 250 mm), and their identities were confirmed by matrix-assisted laser-desorption ionization-time-of-flight mass spectrometry (Shimadzu, Japan). Peptide concentration of the stock solution was determined by measuring absorbance at 280 nm.

Liposome Preparation

Egg phosphatidylcholine/phosphatidylglycerol (ePC/ePG, 2 : 1 molar ratio) vesicles were prepared by dissolving lipids in a methanol–choloroform 1 : 1 mixture. The solvent was then evaporated in a rotary vacuum system, until a thin film was formed. The lipid film was dried under vacuum for at least 2 h and then hydrated with a physiological buffer (phosphate 10 mM, NaCl 140 mM, pH 7.4). After 10 freeze–thaw cycles, liposomes were extruded with a Liposofast Extruder (Avestin GMBH, Mannheim, Germany) through two stacked polycarbonate membranes with pores 100 nm in diameter. The final lipid concentration was estimated using Stewart's phospholipid assay [35].

The degree of labeling of nitroxide-containing lipids (1-palmitoyl-2-stearoyl(*n*-doxyl)-*sn*-glycero-3-phosphocholine, with $n = 5, 7, 10, 12, 16$ and 1,2-diacyl-*sn*-glycero-3-phosphotempocholine), employed for depth-dependent quenching studies, was determined by double integration of electron paramagnetic resonance (EPR) spectra [36]. Nitroxide-labeled liposomes were produced by adding the labeled lipids to the initial chloroform solution (7% molar fraction). The final mixture was ePC/ePG/doxyl-PC in 60 : 33 : 7 molar ratios. Spin label content was controlled directly on the final liposomes by double integration of the EPR spectra of an aliquot of the liposomes dissolved in isopropanol. All liposome preparations contained the same amount of spin labels, within a 10% error.

Journal of PeptideScience

For ion-leakage experiments, ePC/ePG lipids (2 : 1 molar ratio) were hydrated with a solution containing Tris buffer (10 mM), pH 7.4, KCl (150 mM), and the SBFI probe (0.5 mM), and extruded through pores of 200 nm diameter. The vesicles were then eluted on a Sephadex G-50 column, in the same buffer, to remove the unencapsulated probe. Finally, liposomes were diluted (to a 30 μM lipid concentration) in a Na^+ containing buffer (10 mM Tris, pH 7.4, 150 mM NaCl).

For fluorescence anisotropy experiments, vesicles were prepared by adding 1% DPH to a 1,2-dimyristoyl-sn-glycero-3-phosphocholine/1,2-dimyristoyl-sn-glycero-3-phospho-(1′-rac-glycerol) (DMPC/DMPG) lipid mixture (2 : 1 molar ratio), before film formation.

Giant unilamellar vesicles (GUVs) were prepared by the electroformation method, as previously described [37]. After lipid film formation on one of the two electrodes, the electroformation chamber was filled with a 0.32 M sucrose solution, and a 1.5 V (peak to peak), 10 Hz potential was applied for 1 h, and then switched to 4 V, 4 Hz for 15 min to favor detachment of GUVs from the electrode. The solution contained in the electroformation chamber was gently removed and diluted 300 times in buffer (pH 7.4, 10 mM phosphate, 198 mM NaCl, 0.1 mM EDTA). The lipid composition of GUVs was 66% ePC, 33% ePG, and 1% rhodamine-labeled phosphatidylethanolamine (Rho-PE). Glass slides employed during fluorescence imaging were previously treated with Sigmacote (Sigma-Aldrich). The FITC-labeled peptide (0.7 μM) and the lipid membrane could be observed independently by imaging the green fluorescein emission and the red Rho-PE fluorescence in a Nikon Ti Eclipse confocal laser-scanning microscope (Nikon, Tokyo, Japan).

Absorbance Measurements

All absorption spectra were collected with a Cary Win-UV spectrophotometer (Varian, Santa Clara, CA, USA). The turbidity at 400 nm was measured by adding increasing lipid concentrations (from 2 to 200 μM) to Pep-1 or to Pep-1-K (1 μM).

Fluorescence Measurements

Fluorescence spectra were performed with a Fluoromax-2 (Jobin-Yvon, Longjumeau, France) spectrofluorimeter using a 1 × 1 cm quartz cell. Water–membrane partition experiments were carried out using a peptide concentration of 1 μM. Emission spectra were collected using $\lambda_{exc} = 280$ nm. In ion-leakage experiments, excitation spectra were collected with $\lambda_{em} = 505$ nm, using a 385 nm cut-off filter, at a lipid concentration of 30 μM. Background caused by peptide-induced liposome aggregation was subtracted by acquiring the same spectra with liposomes not containing the SBFI fluorescent probe.

Fluorescence anisotropy was measured with $\lambda_{exc} = 350$ nm and $\lambda_{em} = 450$ nm, and a 385 nm cut-off filter. Each reported value is the average of nine repeated measurements.

Confocal Laser-scanning Microscopy

Escherichia coli cultures were grown to the mid-logarithmic phase. *E. coli* cells (10^7 CFU/ml) in phosphate-buffered saline (PBS) solution (10 mM phosphate, 140 mM KCl, pH 7.4) were incubated with FITC-labeled peptides (10 μg/ml) at 37 °C for 30 min. Then, cells were rinsed twice with PBS and immobilized on a glass slide. HeLa cells (2×10^5/ml) were plated on a glass coverslip, grown overnight, and then incubated with FITC-labeled peptides (10, 5, or 2.5 μg/ml). The cells were rinsed three times with PBS, and then fixed using 4% paraformaldehyde for 15 min. FITC-labeled peptides were visualized with a Zeiss confocal laser-scanning microscope (Carl Zeiss Germany, Oberkochen, Germany).

Results and Discussion

Cell-penetrating Properties

The cell-penetrating activity of Pep-1-K and Pep-1 was compared by incubating FITC-labeled analogs of the two peptides with both bacterial and eukaryotic cells. The confocal microscopy images reported in Figures 1 and 2 show that both peptides are

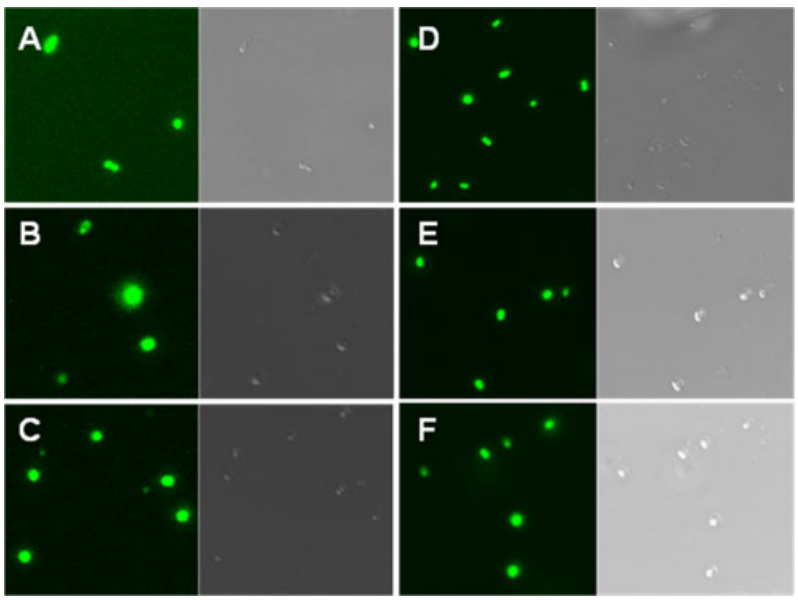

Figure 1. Confocal laser-scanning and DIC microscopy images (left and right panels, respectively) of *Escherichia coli* treated with fluorescein isothiocyanate (FITC)-labeled peptides. Cells were treated with 10 μg/ml of FITC-labeled Pep-1 (A, B and C, representative images of different samples) or FITC-labeled Pep-1-K (D, E and F, representative images of different samples). This figure is available in colour online at wileyonlinelibrary.com/journal/jpepsci.

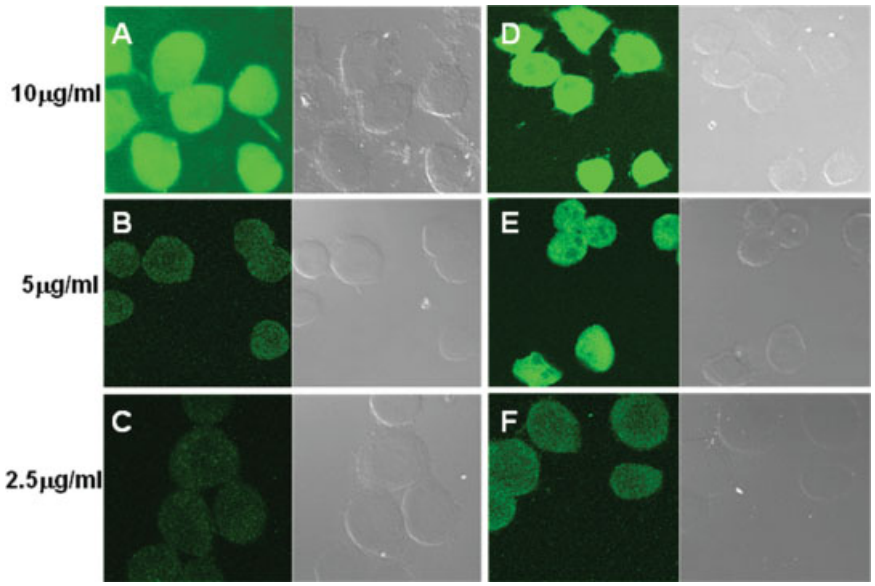

Figure 2. Confocal laser-scanning and DIC microscopy images (left and right panels, respectively) of HeLa cells treated with fluorescein isothiocyanate (FITC)-labeled peptides. Cells were treated with FITC-labeled Pep-1 (A, B and C; 10, 5 and 2.5 μg/ml peptide concentration, respectively) and FITC-labeled Pep-1-K (D, E and F; 10, 5 and 2.5 μg/ml peptide concentration, respectively).

internalized in the cells, indicating that the Glu to Lys substitutions in Pep-1-K do not abolish the cell-penetrating activity.

Membrane-perturbing Activity

Neither Pep-1 nor Pep-1-K induce any significant leakage of the fluorescent dye carboxyfluorescein from liposomes [33]. However, Pep-1-K, in contrast to Pep-1, appears to induce membrane depolarization in bacteria [33]. This is not necessarily due to a direct membrane effect of Pep-1-K, but could be an indirect consequence of Pep-1-K interaction with some bacterial intracellular target. Another possibility is that Pep-1-K causes the formation of membrane defects or pores, which are too small to cause the leakage of a fluorophore, while being sufficiently large to allow the release of ions. To clarify this point, we studied Pep-1-K-induced ion leakage in artificial membranes, by entrapping a sodium-sensing dye (SBFI) inside lipid vesicles, and including NaCl in the buffer in which these liposomes were suspended. Addition of Pep-1-K caused Na^+ entry into the vesicles, as shown by the change in the SBFI excitation spectrum (Figure 3). By contrast, Pep-1-K was not able to cause such leakage at any concentration tested (up to 10 μM).

More evidence of Pep-1-K-induced membrane perturbation is reported in Figures 4 and 5. The peptide induced significant vesicle aggregation (Figure 4), as shown by the increase in light scattering of a vesicle suspension in the presence of the peptide. This effect was not detected in the presence of Pep-1. Interestingly, the Pep-1-K-induced aggregation was reversible: when the peptide was titrated with increasing vesicle concentrations, aggregation reached a maximum at a lipid to peptide ratio of about 80 and then decreased. This finding can be understood in terms of electrostatic interactions. Peptide binding to the anionic vesicles causes neutralization of vesicle charges and decreases their repulsion, favoring aggregation. As more liposomes are added, the peptides are distributed over more vesicles, and therefore the total negative charge in each liposome increases again, causing a reduction in vesicle aggregation. The reversibility of the increase in light scattering indicates that Pep-1-K is causing vesicle aggregation rather than fusion, and therefore this process is probably not the origin of Pep-1-K-induced ion leakage.

However, another experiment provides evidence that Pep-1-K also induces a significant perturbation of membrane order and dynamics. The fluorescent probe DPH inserts into the hydrophobic core of the membrane, essentially parallel to the lipid chains. For this reason, its fluorescence anisotropy reports on the membrane order and dynamics. As shown in Figure 5, Pep-1-K binding significantly modifies the dynamics of a DMPC/DMPG bilayer both above and below the thermotropic phase transition, while no peptide-induced membrane perturbation was observed for Pep-1 in the physiologically relevant fluid state. Therefore, peptide-induced membrane perturbation could be the basis of the Pep-1-K-induced ion leakage.

Water–membrane Peptide Partition

What is the origin of the increased membrane-perturbing activity of Pep-1-K, as compared to Pep-1? To answer this question, the affinity of Pep-1-K and Pep-1 for lipid bilayers mimicking the composition of bacterial membranes was investigated by measuring the changes in the emission spectrum of the peptides caused by titration of a peptide solution with ePC/ePG liposomes. Membrane binding caused a significant blue shift in the emission spectrum of both peptides, due to the change in the polarity of the environment of the Trp residues [38]. As shown in Figure 6, Pep-1-K exhibited a significantly higher affinity for membranes than Pep-1. On the other hand, the spectral shift caused by membrane association was similar for both peptides, suggesting that they have a similar position and orientation in the membrane. These findings indicate that the higher antibacterial activity of Pep-1-K is likely due, at least in part, to its higher membrane affinity.

Direct observation of Pep-1-K association to membranes was possible using a fluorescein-labeled analog and GUVs. As shown in Figure 7, Pep-1-K localizes almost exclusively on the membrane surface, with negligible peptide fluorescence in the water phase

Journal of PeptideScience

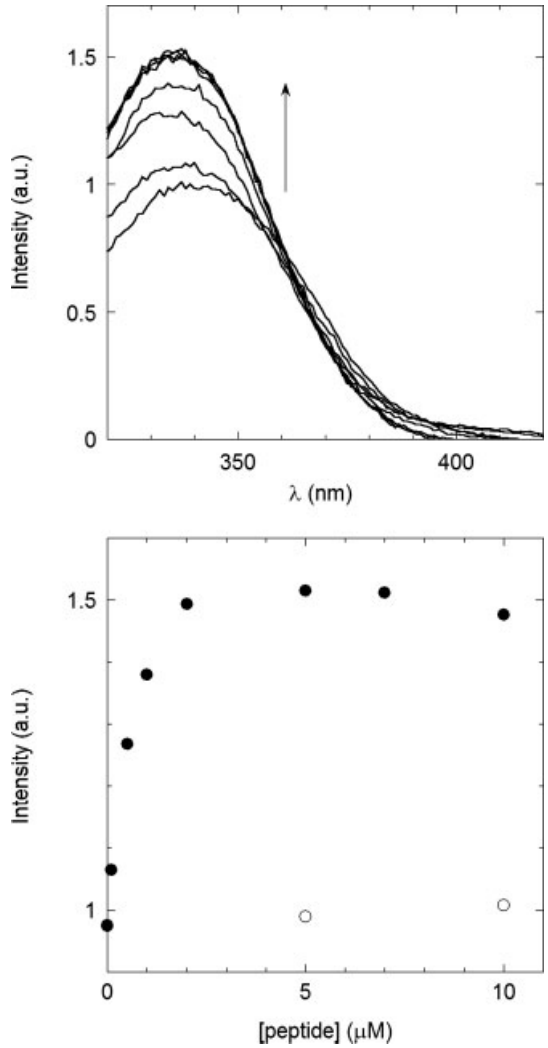

Figure 3. Peptide-induced membrane permeability to ions, followed by the variation in the excitation spectrum of the sodium-sensitive dye sodium-binding benzofuran isophthalate, entrapped inside vesicles. Liposomes were suspended in a buffer containing NaCl 150 mM, while KCl 150 mM was included in the buffer entrapped inside vesicles. Upper panel: excitation spectra measured after addition of different Pep-1-K concentrations (0.1–10 μM). The arrow indicates increasing peptide concentration. Lower panel: fluorescence intensity at λ_{ex} = 335 nm, as a function of peptide concentration. Full symbols: Pep-1-K; empty symbols: Pep-1. λ_{em} = 505 nm. Egg phosphatidylcholine/phosphatidylglycerol (ePC/ePG) 2 : 1 (mol/mol) vesicles, [lipid] = 30 μM.

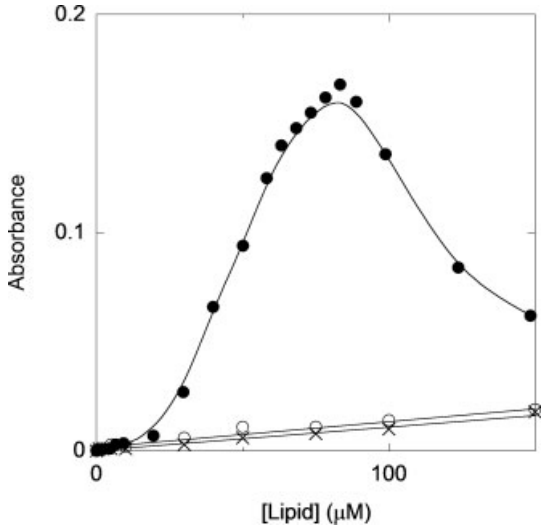

Figure 4. Peptide-induced vesicle aggregation, as measured by the sample turbidity at 400 nm. Empty circles: peptide-free sample; full circles: Pep-1-K-containing sample; crosses: Pep-1-containing sample. [Peptide] = 1 μM. Egg phosphatidylcholine/phosphatidylglycerol (ePC/ePG) 2 : 1 (mol/mol) vesicles.

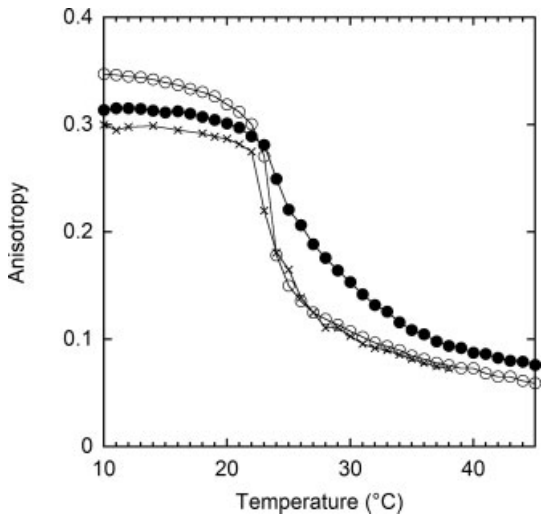

Figure 5. Effect of peptide–membrane interaction on the thermotropic phase transition of 1,2-dimyristoyl-sn-glycero-3-phosphocholine/1,2-dimyristoyl-sn-glycero-3-phospho-(1′-rac-glycerol) (DMPC/DMPG) vesicles, as followed by the fluorescence anisotropy of 1,6-diphenyl-1,3,5-hexatriene (DPH). Empty circles: peptide-free vesicles; filled circles: Pep-1-K-associated vesicles; crosses: Pep-1-associated vesicles DMPC/DMPG 2 : 1 (mol/mol), DPH 1%, [lipid] = 50 μM; [Peptide] = 10 μM.

both outside and inside GUVs. Surprisingly, Pep-1-K did not associate homogeneously to all vesicles, but this could be due to the impossibility of stirring the sample when the peptide was added in the observation chamber. On the other hand, the fact that the peptide did not translocate to the inner aqueous volume of these artificial vesicles was not unexpected, as even in the case of Pep-1 a transmembrane potential is needed for the cell-penetrating activity [39].

Peptide Location in the Bilayer

Peptide location in the membrane was determined by depth-dependent quenching experiments [36,38]. Figure 8 shows the peptide fluorescence quenching caused by association to liposomes containing lipids labeled at different depths along the acyl chain with a doxyl group, which acts as a quencher of peptide Trp fluorescence. Surprisingly, the quenching profile was rather well defined, notwithstanding the presence of 5 Trp residues in the peptide sequence. This result indicates that all fluorophores are located at a similar depth in the membrane, approximately 11–12 Å from the bilayer center, i.e. just below the phospholipid headgroups [40]. Therefore, the peptide is oriented essentially parallel to the membrane surface, and this orientation does not change with peptide concentration (within the range investigated). This position and orientation suggest a mechanism of membrane perturbation that could be described according to the 'carpet' model [7].

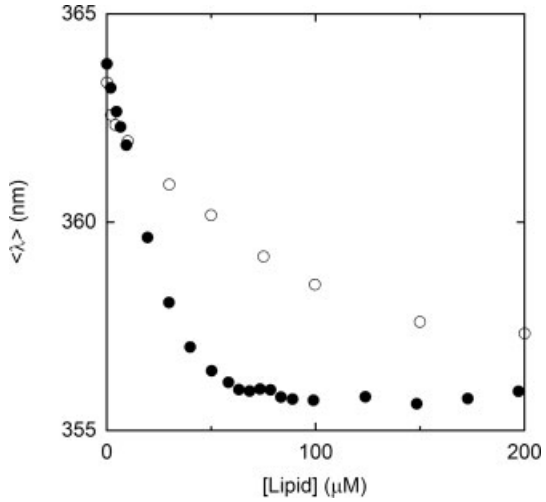

Figure 6. Water to membrane partition of Pep-1 (empty symbols) and Pep-1-K (filled symbols), followed by the shift in the fluorescence emission spectrum. [Peptide] = 1 μM, Egg phosphatidylcholine/phosphatidylglycerol (ePC/ePG) 2 : 1 (mol/mol) vesicles, λ_{exc} = 280 nm, λ_{em} = 320–420 nm.

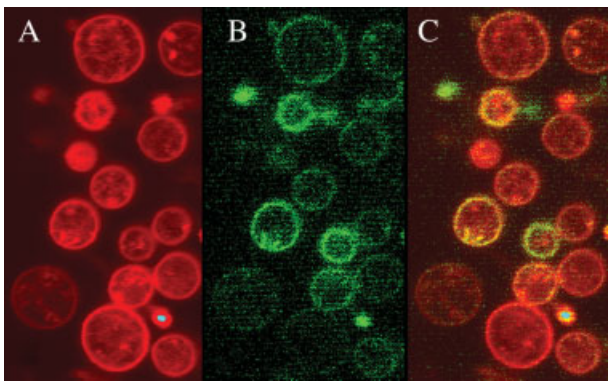

Figure 7. Association of fluorescein-labeled Pep-1-K (3 μM) with rhodamine-labeled giant unilamellar vesicles (GUVs). Panel A: lipid fluorescence. Panel B: Pep-1-K fluorescence. Panel C: overlap of the two images reported in panels A and B. Image size 37.5 × 75 μm. GUV composition: egg phosphatidylcholine/phosphatidylglycerol/rhodamine-labeled phosphatidylethanolamine (ePC/ePG/Rho-PE) 66 : 33 : 1 (molar ratios).

Conclusions

Our data indicate that the main difference between Pep-1 and Pep-1-K is in their relative affinities toward bacterial membranes: Pep-1-K binds to anionic bilayers more strongly, due to its higher cationic charge. This conclusion is in agreement with the correlation recently shown between water–membrane partition constants and MIC values of AMPs [41]. In the 'carpet' model of peptide-induced membrane perturbation, AMPs need to reach a threshold of membrane-bound peptide concentration before they can cause the formation of defects or pores resulting in membrane leakage. Therefore, it is evident that the higher the peptide affinity toward bacterial membranes, the lower is the concentration needed to reach this threshold. Our data are consistent with a 'carpet' model of membrane perturbation by Pep-1-K: it binds to the membrane surface and perturbs the order of the bilayer. This leads to the leakage of ions, but not of larger molecules, at least in the concentration range investigated. The ability of Pep-1-K

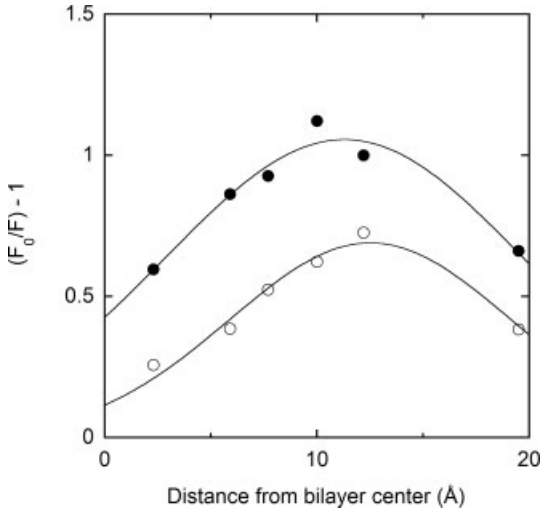

Figure 8. Depth-dependent quenching experiment to determine the position of Pep-1-K in the membrane. [Peptide] = 1 μM (full symbols) or 10 μM (empty symbols), [lipid] = 200 μM. *F* and F_0 are the fluorescence intensities measured for the peptide associated to doxyl-labeled and unlabeled membranes, respectively. λ_{exc} = 280 nm, λ_{em} = 320–420 nm. Egg phosphatidylcholine/phosphatidylglycerol (ePC/ePG, 2 : 1, mol/mol) vesicles, doxyl-labeled lipid content 7%.

to depolarize bacterial cells is very likely due to the membrane disorder it causes when it binds to their membrane surface.

Apparently, the change in membrane affinity caused by the Glu to Lys substitutions in Pep-1-K, while increasing its membrane-perturbing activity, does not inhibit its cell-penetrating properties. This is not surprising, as also the high translocation efficiency of Pep-1 itself has been shown to be linked to its strong affinity toward cellular membranes [29].

In conclusion, the example of Pep-1 and Pep-1-K clearly illustrates that CPPs and AMPs are not two separate classes, as subtle modifications can determine which of the two activities predominates.

References

1 Castanho MARB. *Membrane-active Peptides: Methods and Results on Structure and Function*. International University Line: La Jolla, CA, 2009.
2 Steiner H, Hultmark D, Engström A, Bennich H, Boman HG. Sequence and specificity of two antibacterial proteins involved in insect immunity. *Nature* 1981; **292**: 246–248.
3 Selsted ME, Brown DM, DeLange RJ, Lehrer RI. Primary structures of MCP-1 and MCP-2, natural peptide antibiotics of rabbit lung macrophages. *J. Biol. Chem.* 1983; **258**: 11485–14489.
4 Zasloff M. Magainins, a class of antimicrobial peptides from *Xenopus* skin: isolation, characterization of two active forms and partial cDNA sequence of a precursor. *Proc. Natl. Acad. Sci. U.S.A.* 1987; **84**: 5449–5454.
5 Lai Y, Gallo RL. AMPed up immunity: how antimicrobial peptides have multiple roles in immune defense. *Trends Immunol.* 2009; **30**: 131–141.
6 Auvynet C, Rosenstein Y. Multifunctional host defense peptides: antimicrobial peptides, the small yet big players in innate and adaptive immunity. *FEBS J.* 2009; **276**: 6497–6508.
7 Shai Y. Mode of action of membrane active antimicrobial peptides. *Biopolymers* 2002; **66**: 236–248.
8 Bocchinfuso G, Palleschi A, Orioni B, Grande G, Formaggio F, Toniolo C, Park Y, Hahm KS, Stella L. Different mechanisms of action of antimicrobial peptides: insights from fluorescence spectroscopy

experiments and molecular dynamics simulations. *J. Pept. Sci.* 2009; **15**: 550–558.
9 Steinstraesser L, Kraneburg UM, Hirsch T, Kesting M, Steinau HU, Jacobsen F, Al-Benna S. Host defense peptides as effector molecules of the innate immune response: a sledgehammer for drug resistance?. *Int. J. Mol. Sci.* 2009; **10**: 3951–3970.
10 Pathan FK, Venkata DA, Panguluri SK. Recent patents on antimicrobial peptides. *Recent Pat. DNA Gene Seq.* 2010; **4**: 10–16.
11 Frankel AD, Pabo CO. Cellular uptake of the tat protein from human immunodeficiency virus. *Cell* 1988; **55**: 1189–1193.
12 Joliot A, Pernelle C, Deagostini-Bazin H, Prochiantz A. Antennapedia homeobox peptide regulates neural morphogenesis. *Proc. Natl. Acad. Sci. U.S.A.* 1991; **88**: 1864–1868.
13 Langel Ü. *Handbook of Cell Penetrating Peptides*. CRC Press: Oxford, 2006.
14 Heitz F, Morris MC, Divita G. Twenty years of cell-penetrating peptides: from molecular mechanisms to therapeutics. *Br. J. Pharmacol.* 2009; **157**: 195–206.
15 Foerg C, Merkle HP. On the biomedical promise of cell penetrating peptides: limits versus prospects. *J. Pharm. Sci.* 2008; **97**: 144–162.
16 Henriques ST, Melo MN, Castanho MARB. Cell-penetrating peptides and antimicrobial peptides: how different are they?. *Biochem. J.* 2006; **399**: 1–7.
17 Nekhotiaeva N, Elmquist A, Kuttuva Rajarao G, Hällbrink M, Langel Ü, Good L. Cell entry and antimicrobial properties of eukaryotic cell-penetrating peptides. *FASEB J.* 2004; **18**: 394–396.
18 Palm C, Netzereab S, Hällbrink M. Quantitatively determined uptake of cell-penetrating peptides in non-mammalian cells with an evaluation of degradation and antimicrobial effects. *Peptides* 2006; **27**: 1710–1716.
19 Yandek LE, Pokorny A, Florén A, Knoelke K, Langel Ü, Almeida PFF. Mechanism of the cell-penetrating peptide transportan 10 permeation of lipid bilayers. *Biophys. J.* 2007; **92**: 2434–2444.
20 Thorén PEG, Persson D, Lincoln P, Nordén B. Membrane destabilizing properties of cell-penetrating peptides. *Biophys. Chem.* 2005; **114**: 169–179.
21 Mishra A, Gordon VD, Yang L, Coridan R, Wong GCL. HIV TAT forms pores in membranes by inducing saddle-splay curvature: potential role of bidentate hydrogen bonding. *Angew. Chem. Int. Ed.* 2008; **47**: 2986–2989.
22 Zhu WL, Shin SY. Effects of dimerization of the cell-penetrating peptide Tat analog on antimicrobial activity and mechanism of bactericidal action. *J. Pept. Sci.* 2009; **15**: 345–352.
23 Ciobanasu C, Siebrasse JP, Kubitscheck U. Cell-penetrating HIV1 TAT peptides can generate pores in model membranes. *Biophys. J.* 2010; **99**: 153–162.
24 Zhu WL, Shin SY. Antimicrobial and cytolytic activities and plausible mode of bactericidal action of the cell penetrating peptide penetratin and its Lys-linked two-stranded peptide. *Chem. Biol. Drug Des.* 2009; **73**: 209–215.
25 Park CB, Kim HS, Kim SC. Mechanism of action of the antimicrobial peptide buforin II: buforin II kills microorganisms by penetrating the cell membrane and inhibiting cellular functions. *Biochem. Biophys. Res. Commun.* 1998; **244**: 253–257.
26 Nicolas P. Multifunctional host defense peptides: intracellular-targeting antimicrobial peptides. *FEBS J.* 2009; **276**: 6483–6496.
27 Takeshima K, Chikushi A, Lee K-K, Yonehara S, Matsuzaki K. Translocation of analogues of the antimicrobial peptides magainin and buforin across human cell membranes. *J. Biol. Chem.* 2003; **278**: 1310–1315.
28 Morris MC, Depollier J, Mery J, Heitz F, Divita G. A peptide carrier for the delivery of biologically active proteins into mammalian cells. *Nat. Biotech.* 2001; **19**: 1173–1176.
29 Henriques ST, Castanho MARB, Pattenden LK, Aguilar M. Fast membrane association is a crucial factor in the peptide Pep-1 translocation mechanism: a kinetic study followed by surface plasmon resonance. *Biopolymers (Pept. Sci.)* 2010; **94**: 314–322.
30 Muñoz-Morris MA, Heitz F, Divita G, Morris MC. The peptide carrier Pep-1 forms biologically efficient nanoparticle complexes. *Biochem. Biophys. Res. Commun.* 2007; **355**: 877–882.
31 Deshayes S, Plénat T, Charnet P, Divita G, Molle G, Heitz F. Formation of transmembrane ionic channels of primary amphipathic cell-penetrating peptides. Consequences on the mechanism of cell penetration. *Biochim. Biophys. Acta* 2006; **1758**: 1846–1851.
32 Henriques ST, Castanho MARB. Translocation or membrane disintegration? Implication of peptide–membrane interactions in pep-1 activity. *J. Pept. Sci.* 2008; **14**: 482–487.
33 Zhu WL, Lan H, Park I-S, Kim JI, Jin HZ, Hahm K-S, Shin SY. Design and mechanism of action of a novel bacteria-selective antimicrobial peptide from the cell-penetrating peptide Pep-1. *Biochim. Biophys. Res. Commun.* 2006; **349**: 769–774.
34 Park N, Yamanaka K, Tran D, Chandrangsu P, Akers JC, de Leon JC, Morrissette NS, Selsted ME, Tan M. The cell-penetrating peptide, Pep-1, has activity against intracellular chlamydial growth but not extracellular forms of *Chlamydia trachomatis*. *J. Antimicrob. Chemother.* 2009; **63**: 115–123.
35 Stewart JCM. Colorimetric determination of phospholipids with ammonium ferrothiocyanate. *Anal. Biochem.* 1980; **104**: 10–14.
36 Chattopadhyay A, London E. Parallax method for direct measurement of membrane penetration depth utilizing fluorescence quenching by spin-labeled phospholipids. *Biochemistry* 1987; **26**: 39–45.
37 Stella L, Pallottini V, Moreno S, Leoni S, De Maria F, Turella P, Federici G, Fabrini R, Dawood KF, Lo Bello M, Pedersen JZ, Ricci G. Electrostatic association of glutathione transferase to the nuclear membrane. Evidence of an enzyme defense barrier at the nuclear envelope. *J. Biol. Chem.* 2007; **282**: 6372–6379.
38 Stella L, Venanzi M, Hahm KS, Formaggio F, Toniolo C, Pispisa B. Shining a light on peptide-lipid interactions. Fluorescence methods in the study of membrane-active peptides. *Chem. Today* 2008; **26**: 44–46.
39 Henriques ST, Castanho MARB. Consequences of nonlytic membrane perturbation to the translocation of the cell penetrating peptide Pep-1 in lipidic vesicles. *Biochemistry* 2004; **43**: 9716–9724.
40 Orioni B, Bocchinfuso G, Kim JY, Palleschi A, Grande G, Bobone S, Park Y, Kim JI, Hahm KS, Stella L. Membrane perturbation by the antimicrobial peptide PMAP-23: a fluorescence and molecular dynamics study. *Biochim. Biophys. Acta* 2009; **1788**: 1523–1533.
41 Melo MN, Ferre R, Castanho MARB. Antimicrobial peptides: linking partition, activity and high membrane-bound concentrations. *Nat. Rev. Microbiol.* 2009; **7**: 245–250.

